Diffractive optical elements for spectral imaging

Daniel W. Wilson, Paul D. Maker, Richard E. Muller, and Pantazis Mouroulis
Jet Propulsion Laboratory, California Institute of Technology, MS 302-231, 4800 Oak Grove Drive, Pasadena, CA 91109
Tel: (818) 393-3548, Fax: (818) 393-4540, E-mail: daniel.w.wilson@jpl.nasa.gov

Michael R. Descour, Curtis E. Volin, and Eustace L. Dereniak
Optical Sciences Center, University of Arizona, Tucson, AZ 85721
Tel: (520) 626-5086, Fax: (520) 621-3389, E-mail: michael.descour@opt-sci.arizona.edu

Abstract: Diffractive optical elements fabricated on flat and non-flat substrates frequently act as dispersive elements in imaging spectrometers. We describe the design and electron-beam fabrication of blazed and computer-generated-hologram gratings for slit and tomographic imaging spectrometers.

OCIS codes: (050.1950) Diffraction gratings, (220.4000) Microstructure fabrication

1. Convex blazed gratings for slit imaging spectrometers

The dispersive element in many slit imaging spectrometers is a blazed grating. In recent years, the concentric "Offner" [1] spectrometer design (Fig. 1) has become popular due to its very low slit distortion [2,3]. This design requires the grating to be fabricated on a spherical convex substrate. For high efficiency, the grating must be blazed. However, the non-flat substrate requirement makes diamond ruling difficult, and the blazing requirement makes holographic fabrication difficult. To address this need, we have developed an analog direct-write electron-beam lithography method for fabricating high-efficiency blazed gratings on convex substrates [4,5].

Since 1992, we have been using direct-write electron-beam lithography to fabricate analog-depth diffractive optics in thin films of polymethyl methacrylate (PMMA). As detailed in Ref. 6, the process involves determining the proper E-beam dose to a produce a desired etch depth after acetone development. This calculation includes the experimentally determined backscattered dose from the substrate (proximity effect) and the nonlinear dose response of PMMA. For diffractive optic fabrication on non-flat (to date convex spherical) substrates, we utilize the large depth-of-field inherent in E-beam lithography. By careful calibration and testing, we have found that fabrication errors are negligible over regions that vary by ±25 μm in height. To accommodate larger height variations, the total pattern is divided into sub-patterns (annuli) with height variations of 50 μm. Each sub-pattern is exposed using the proper settings for E-beam focus height, deflector gain, and deflector rotation. Figure 2 shows an atomic force microscope scan of a typical blazed grating.

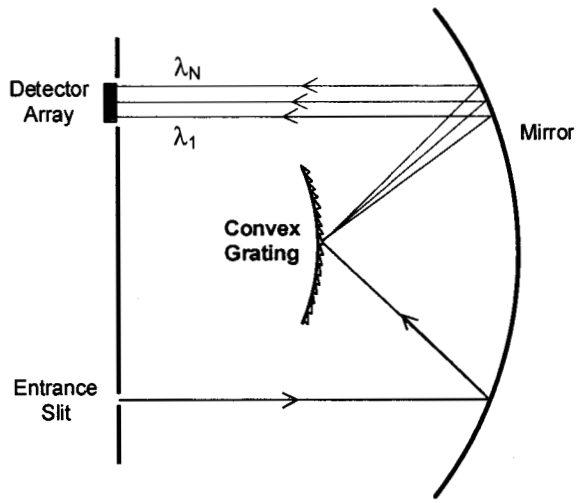

Fig. 1. Illustration of Offner imaging spectrometer form

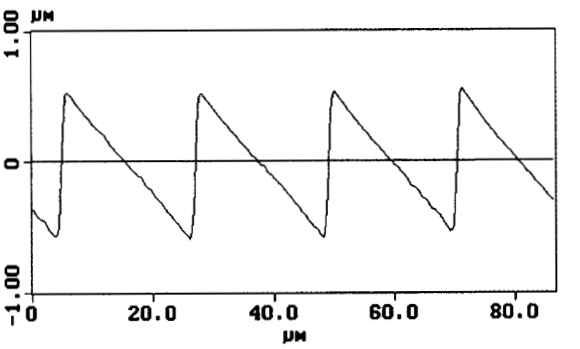

Fig. 2. Typical groove profile of an E-beam fabricated blazed grating (atomic force microscope scan)

Since 1998, we have delivered space-qualified gratings for imaging spectrometers in two flight instruments. Table 1 summarizes the specifications and measured performance of these gratings. For both of these instruments, the substrates were polished aluminum that we coated with 2 μm of PMMA. After grating fabrication, we evaporated 600Å of aluminum as the reflective surface. In all cases, the measured efficiency curve shapes matched theoretical predictions for a sawtooth groove profile.

Table 1. Specifications and performance of flight-instrument gratings

Grating	Diameter	Period	Blaze Angle	Substrate Sag	Wavelength range (order)	Peak Efficiency†, Wavelength (order)	Ghosts, Scatter‡
Spect. 1 VNIR	14 mm	17.4 μm	0.55 deg	0.23 mm	0.4 – 0.85 μm (-1)	92% @ 490 nm	0.025%
Spect. 1 SWIR	14 mm	17.4 μm	2.27 deg	0.23 mm	1.13 – 2.55 μm (-1)	92% @ 1450 nm	0.16%
Spect. 2 Dual-band	29 mm	35.7 μm	1.19 deg	1.27 mm	0.5 – 0.85 (-2) 1.0 – 2.45 (-1)	91% @ 0.63 μm (-2) 93% @ 1.26 μm (-1)	0.05%
Spect. 2 MWIR	36.6 mm	103.6 μm	1.12 deg	0	3 – 5 μm (-1)	Not Meas.	Not Meas.

† - relative to an aluminum mirror

‡ - compared to the brightest order at 633 nm, in all cases ghosts dominated over diffuse scatter

For imaging spectrometers operating at shorter wavelengths or requiring higher dispersion, we have begun fabricating blazed gratings with smaller periods. Figure 2 shows a scanning electron microscope image of a 0.5 μm period blazed grating (2000 lines/mm).

Fig. 3. SEM image of PMMA blazed grating with 0.5 μm period.

2. Computer-generated hologram gratings for tomographic imaging spectrometers

In addition to traditional blazed grating profiles, we have designed and fabricated two-dimensional computer-generated hologram (CGH) gratings for computed-tomography imaging spectrometers (CTISs). The CTIS enables transient-event spectral imaging by capturing spatial and spectral information in a single image [7]. This is accomplished by imaging a scene through a 2D grating that produces multiple spectrally dispersed images. These images are simultaneously recorded by a focal plane array (FPA). From a single captured frame, tomographic reconstruction yields the spectrum of every pixel in the scene.

The two-dimensional grating in a CTIS is essentially a 1 to N×N fan-out CGH that is designed to operate over a wide wavelength range. The grating is composed of M×M-pixel CGH cells (M>N) that are arrayed to fill the desired aperture. When illuminated with broadband light, the grating diffracts efficiently into N×N orders, where the (0,0) order is an undispersed image of the scene and all other orders are dispersed radially. Figure 4 shows a CTIS image of a scene composed of light emitting diodes and laser spots. When designing the CTIS CGH grating, the goal is to fill the FPA with dispersed information without having a single grating order saturate the image. The weighting factors of the N×N orders of the desired fan-out are adjusted so that after dispersion, their intensities will be approximately equal. To design the broadband CGH, we have developed two methods: multiple iterative Fourier transform (IFT) [8] and singular value decomposition (SVD). In the multiple IFT method, we perform many IFT single-wavelength designs of the desired N×N CGH and evaluate the broadband performance of each using a merit function. Because the starting phase function for each design is randomly chosen, the broadband performance can

vary greatly from design to design. The SVD design algorithm directly searches for a solution using "phase modes" of the hologram structure. Each phase mode maps to a change in the diffraction efficiencies, so that a small change in the mode produces a small, nearly linear change in the diffraction pattern. Multi-chromatic design is made possible by a simple generalization of the phase modes to changes in diffraction efficiencies at multiple wavelengths. Figure 5 shows the diffraction efficiencies and dispersed FPA images of a 5×5 equal-efficiency CGH grating designed using the SVD technique.

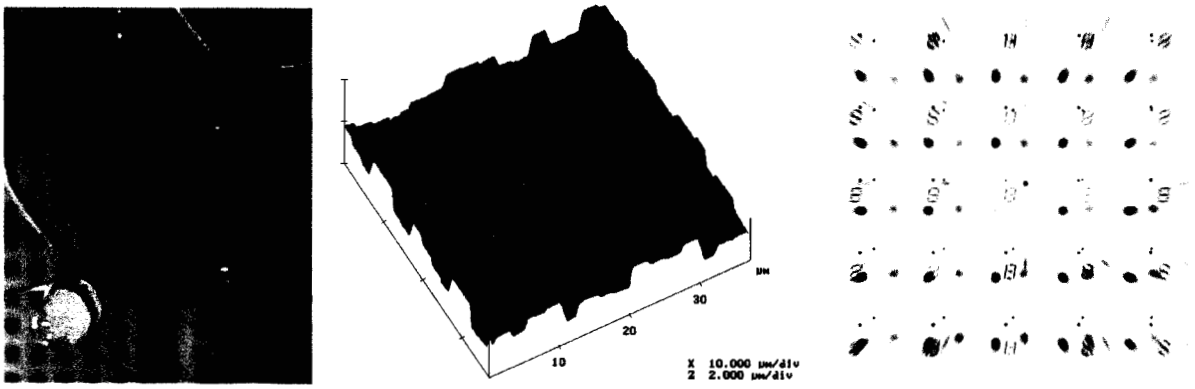

Fig. 4. Left to right: experimental scene, analog-depth E-beam fabricated CGH grating having 2.5 μm pixels (designed to produce 5×5 non-equal efficiency orders for 450-750 nm), CTIS dispersed image using the 5×5 CGH grating.

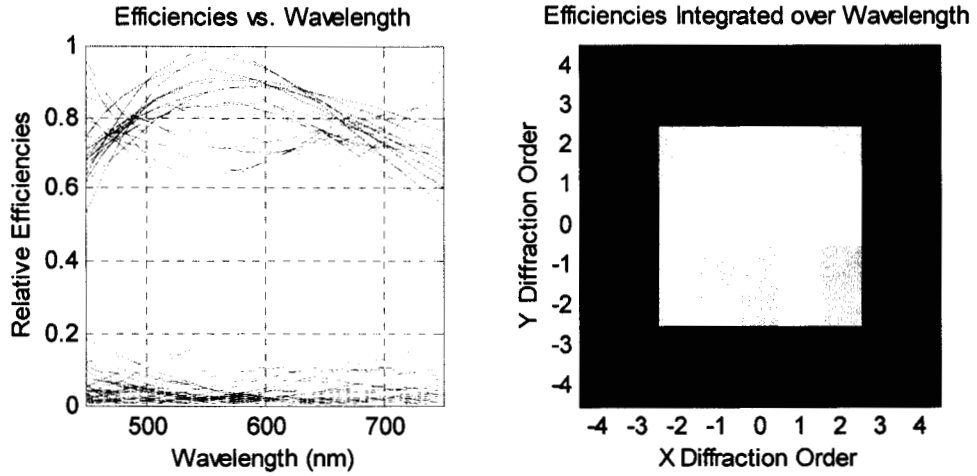

Fig. 5. Predicted relative efficiencies of an equal-efficiency 5×5-order CTIS CGH grating designed using the SVD method.

7. References

[1] A. Offner, "Unit power imaging catoptric anastigmat," U.S. Patent No. 3,748,015 (1973).

[2] M. Chrisp, "Convex diffraction grating imaging spectrometer," U.S. Patent No. 5,880,834 (1999).

[3] P. Mouroulis, "Low-distortion imaging spectrometer designs utilizing convex gratings," in International Optical Design Conference 1998, L. R. Gardner and K. P. Thompson, eds., Proc. SPIE 3482, 594-601 (1998).

[4] P. D. Maker, R. E. Muller, D. W. Wilson, and P. Mouroulis, "New convex grating types manufactured by electron beam lithography," in Diffractive Optics and Micro-Optics, Vol. 10 of OSA Technical Digest Series (Optical Society of America, Washington, D.C., 1998), pp. 234-236.

[5] P. Mouroulis, D. W. Wilson, P. D. Maker, and R. M. Muller, "Convex grating types for concentric imaging spectrometers," *Appl. Opt.* **37**, 7200-7208 (1998).

[6] P. D. Maker, D. W. Wilson, and R. E. Muller, "Fabrication and performance of optical interconnect analog phase holograms made be E-beam lithography," in Optoelectronic Interconnects and Packaging, R. T. Chen and P. S. Guilfoyle, eds., Proc. SPIE CR62, 415-430 (1996).

[7] M. R. Descour and E. L. Dereniak, "Computed-tomography imaging spectrometer: experimental calibration and reconstruction results," *Appl. Opt.* **34**, 4817-4826 (1995).

[8] M. R. Descour, C. E. Volin, T. M. Gleeson, E. L. Dereniak, M. F. Hopkins, D. W. Wilson, and P. D. Maker, "Demonstration of a computed-tomography imaging spectrometer using a computer-generated hologram disperser," *Appl. Opt.* **36**, 3694-3698 (1997).

Diffractive Optical Elements for Spectral Imaging

Daniel Wilson, Paul Maker, Richard Muller, and Pantazis Mouroulis
Center for Space Microelectronics Technology
Jet Propulsion Laboratory
California Institute of Technology
Pasadena, California

Michael Descour, Curtis Volin, and Eustace Dereniak
Optical Sciences Center
University of Arizona
Tucson, Arizona

Outline

- Introduction
- Convex blazed gratings for slit imaging spectrometers
  - Offner imaging spectrometer form
  - Analog surface relief fabrication
  - Convex grating fabrication
  - Grating performance
- Computed generated hologram gratings for tomographic imaging spectrometers
  - Computed-tomography imaging spectrometer overview
  - CGH grating designs
  - Fabrication results
  - Example CTIS results
- Conclusion

Imaging Spectrometry

1. Measure the spectra of all pixels in a scene
2. Analyze the spectra to obtain useful information about the scene

Applications

<u>Remote Sensing</u>

- Mineral exploration
- Hazardous waste monitoring
- Crop/forest health
- Fire/Wetlands monitoring

<u>Defense</u>

- Target identification
- Chemical warfare warning

<u>Biology/Medicine</u>

- Abnormal tissue identification
- Fluorescence studies of cellular processes

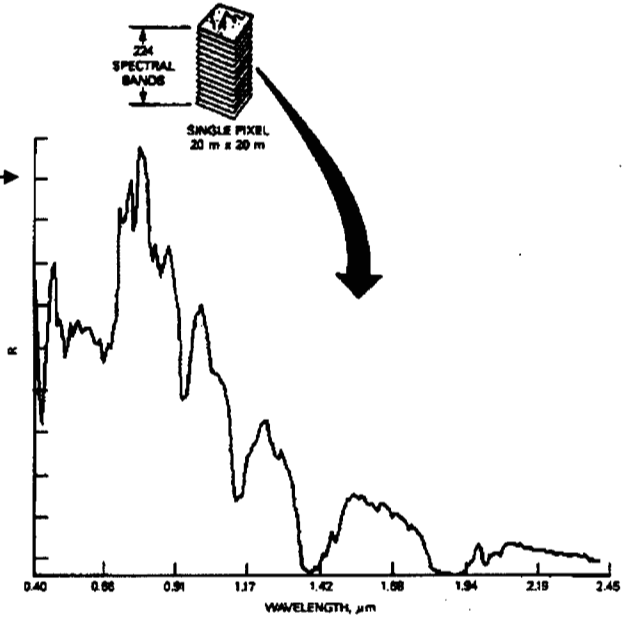

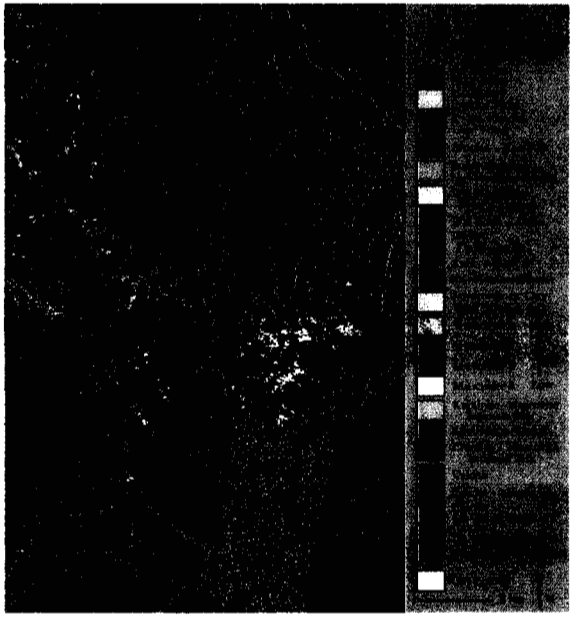

Stationary scene spectral imaging

- Slit imaging spectrometer is used aboard a scanning platform to obtain spectra for a 2D area

Offner Imaging Spectrometer Design

Slit imaging spectrometer based on the Offner concentric two-mirror design

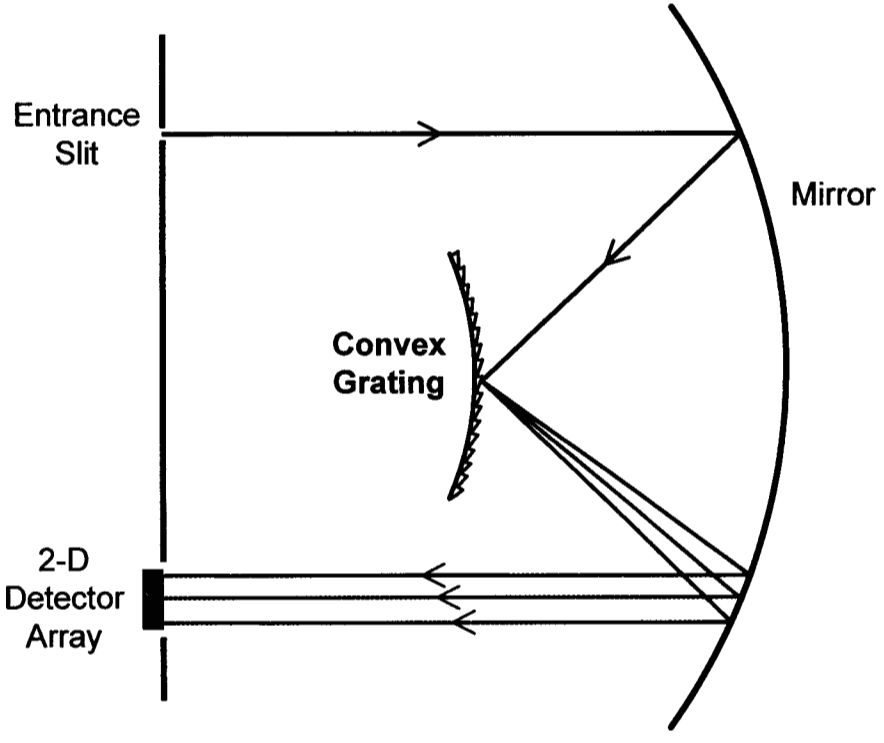

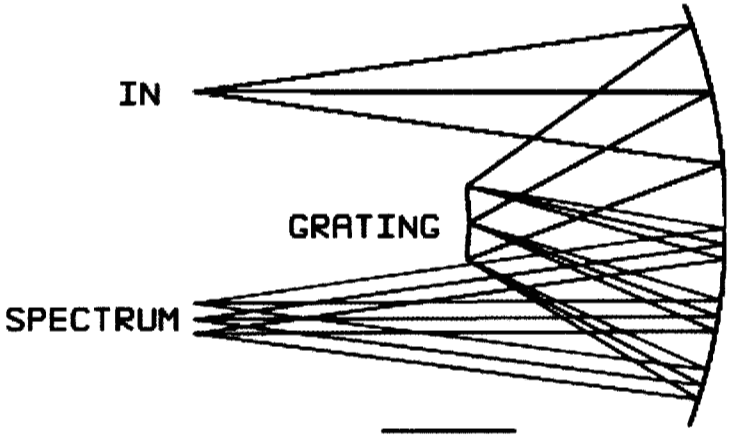

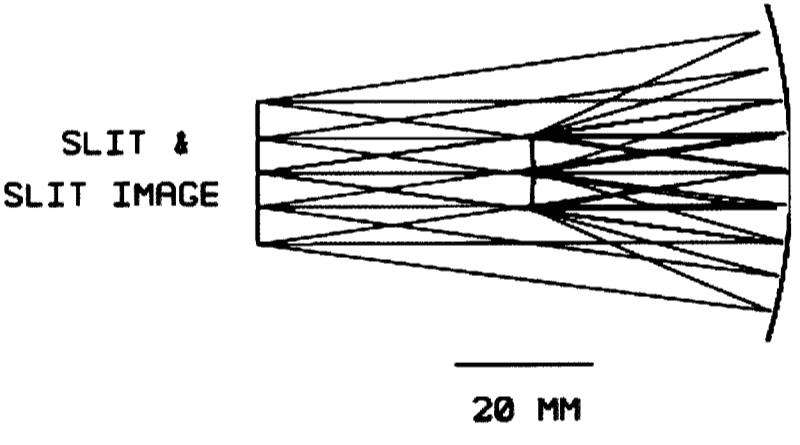

- Can be designed to have *very low slit-image distortion*
  - Minimizes pixel crosstalk
  - Greatly simplifies calibration of the spectrometer
- Near diffraction limited
- Can be very compact and lightweight
- Requires a convex grating (blazed for high efficiency)

E-Beam Fabrication of Analog Diffractive Optics

Fabrication Method

- Thin film of e-beam resist (PMMA or PMGI) spun on substrate
- Direct-write analog-dose electron-beam lithography using JEOL JBX-5DII (50 kV)
- Electron beam breaks bonds in the resist - increases solubility to developer
- Developer etches exposed resist to produce surface relief pattern
- Transfer of patterns into substrate is possible if needed

Advantages

- Well controlled analog depth (< 3% error)
- Arbitrary patterns
- No pattern misalignment
- Prototype elements are efficiently fabricated

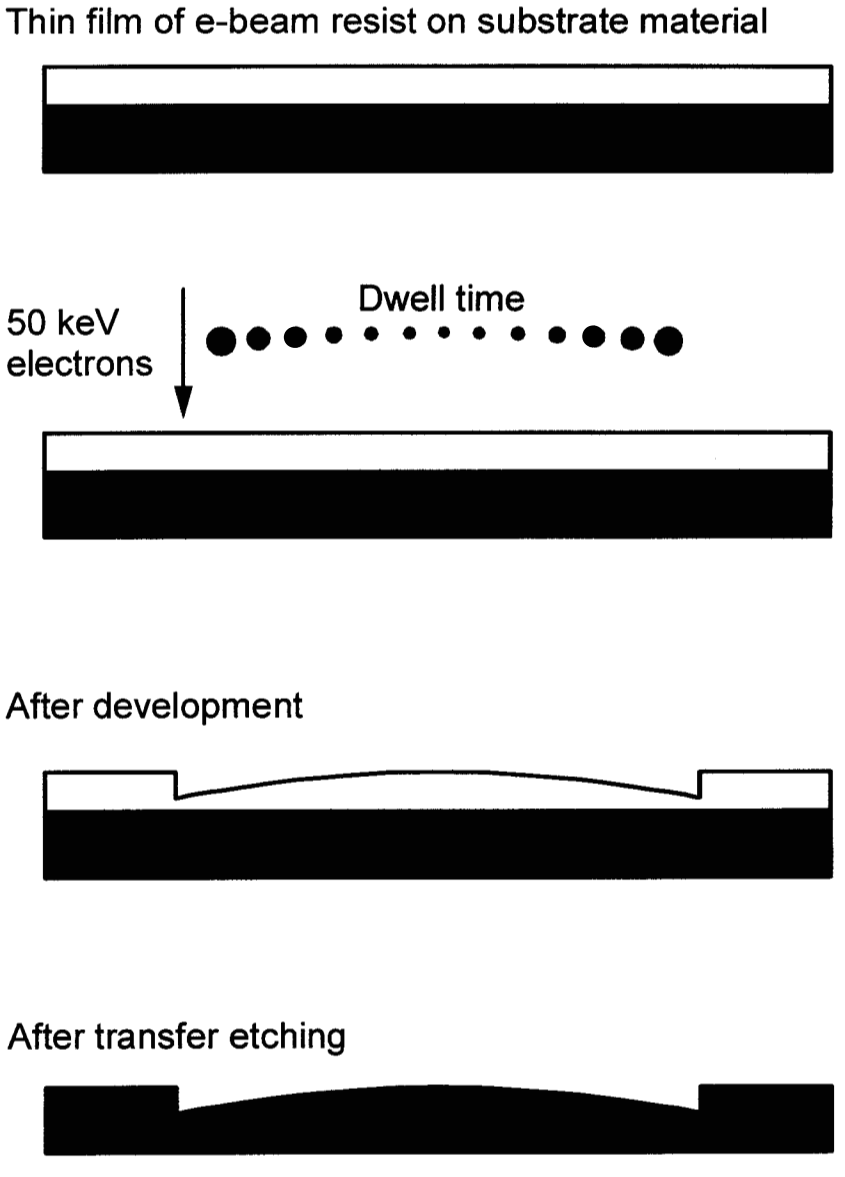

E-Beam Pattern Preparation

- Desired surface relief pattern is represented as square pixels (0.025 - 2.5 microns)
- Pixel depths are converted to E-beam doses using the measured nonlinear dose response of PMMA

$$depth = A + B[\exp(dose/C) - 1], \quad dose = C\ln\left(\frac{depth - A}{B} + 1\right)$$

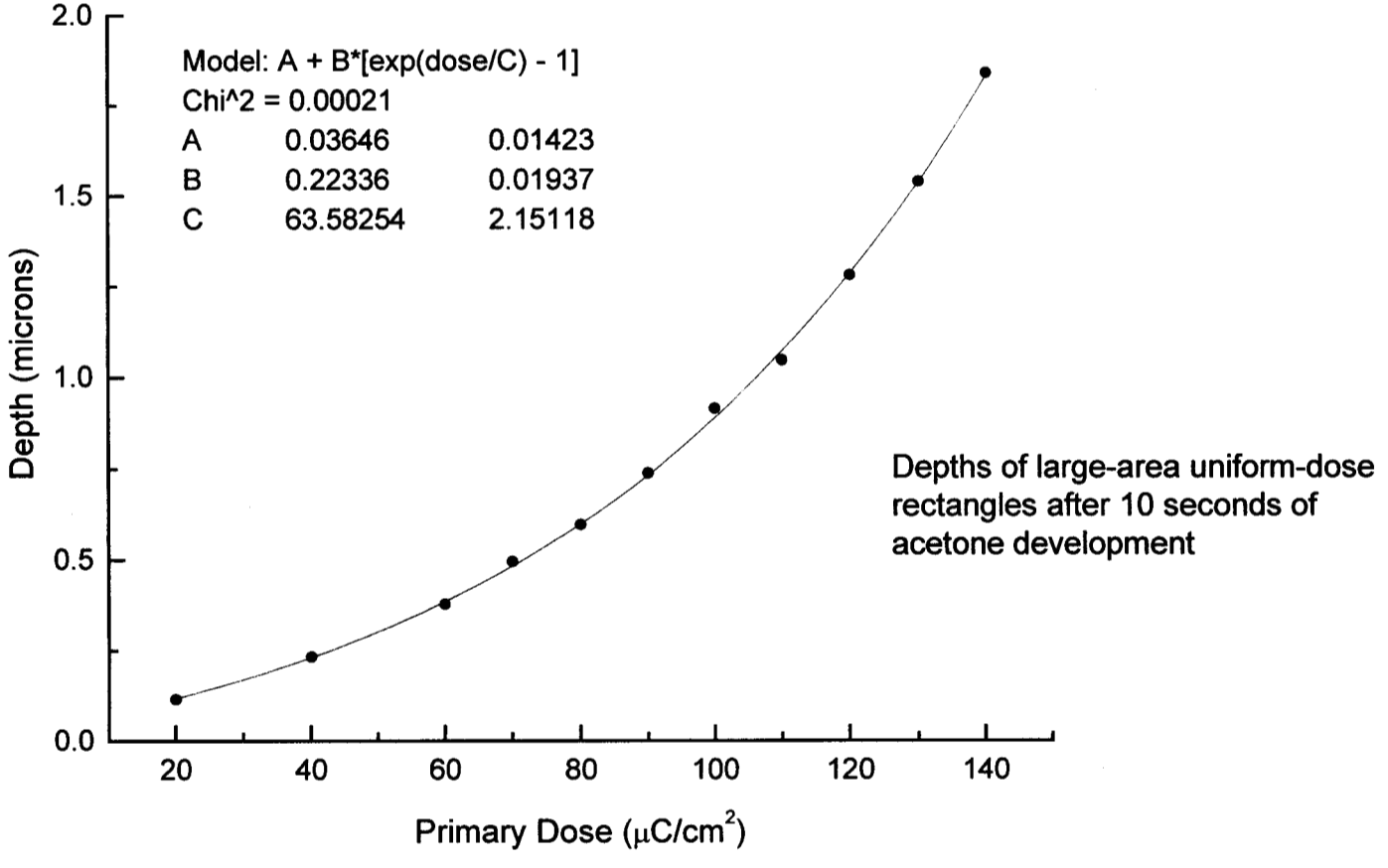

E-Beam Proximity Effect Measurement

- Uniform-dose rectangles are developed for 10 seconds in pure acetone then profiled with an atomic force microscope (AFM)
- Depth profiles are fit with analytical convolution of rectangle with PSF to yield strength η and range α

$$D_{tot} = D_p \,\mathrm{rect}\left(\frac{x}{w}\right) + D_p \frac{\eta}{2}\left[\mathrm{erf}\left(\frac{x+w/2}{\alpha}\right) - \mathrm{erf}\left(\frac{x-w/2}{\alpha}\right)\right], \qquad depth = A + B\left[\exp\left(\frac{D_{tot}}{C(1+\eta)}\right) - 1\right]$$

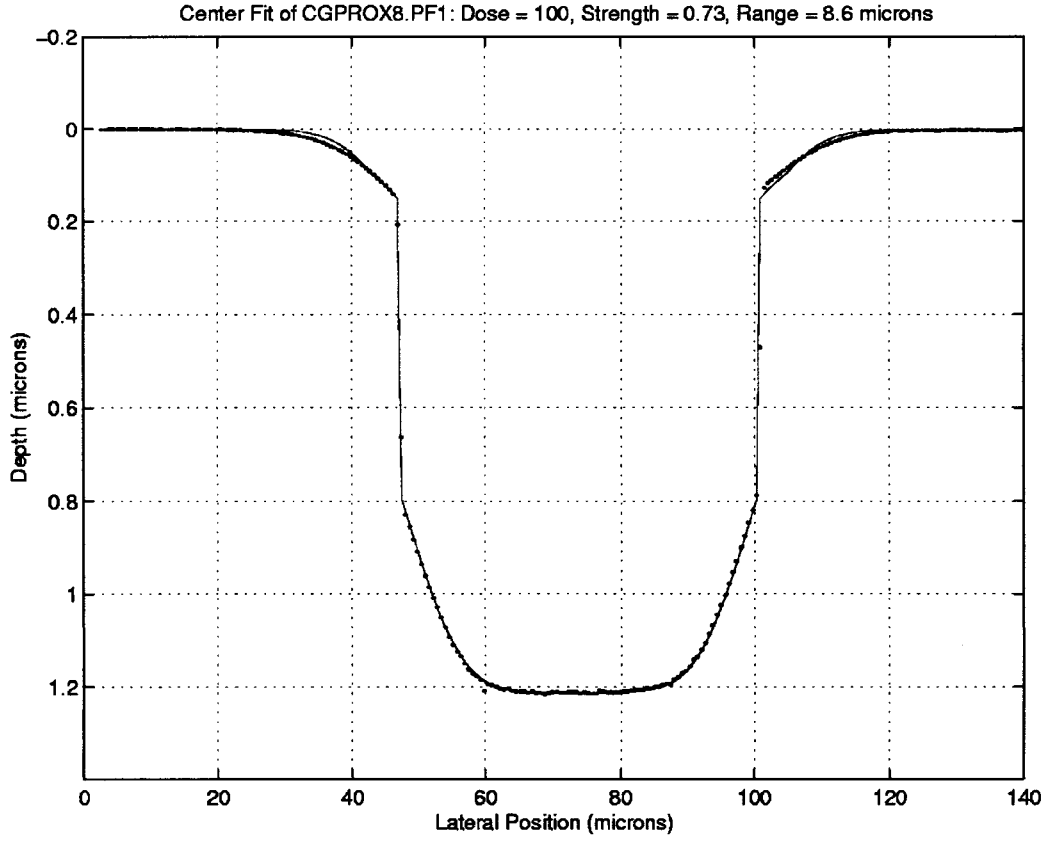

$$PSF(\mathbf{r}) = \delta(\mathbf{r}) + \frac{\eta}{\pi\alpha^2}\exp(-r^2/\alpha^2)$$

Substrate	Strength η	Range α (μm)
Fused Silica	0.50	10.7
Schott CG-455	0.73	8.6
GaAs	0.93	6.0
Aluminum	0.47	9.3

E-Beam Pattern Preparation (continued)

- Proximity effect (dose due to back-scattered electrons) causes neighboring pixels to contribute dose to each other

$$D_{\text{total}}(\mathbf{r}) = D_{\text{primary}}(\mathbf{r}) \otimes PSF(\mathbf{r})$$

$$PSF(\mathbf{r}) = \delta(\mathbf{r}) + \frac{\eta}{\pi\alpha^2}\exp(-r^2/\alpha^2)$$

- Fourier deconvolution is used to correct pixel doses so they produce desired total dose

$$D_{\text{primary}}(\mathbf{r}) = F.T.^{-1}\left\{\frac{F.T.\{D_{\text{total}}(\mathbf{r})\}}{F.T.\{PSF(\mathbf{r})\}}\right\}$$

JPL E-Beam System Specifications

Parameter	***Old → JEOL JBX-5D2***	***New → JEOL JBX-9300FS***	
Voltage	50 kV	100 kV	50 kV
Minimum Spot Size	8 nm	4 nm	7 nm
Beam Current for: 100 nm spot	10 nA	175 nA	125 nA
10 nm spot	10 pA	10 nA	4 nA
Field Size	80 μm	500 μm	1000 μm
Pattern Generator Speed	2 MHz	25 MHz	
Field Stitching Accuracy	75 nm 3σ	20 nm 3σ	
Write Area	5 in sq	9 in sq	
Wafer Size	5 in dia	12 in dia	
Writing Grid	25 A	10 A	
Electron Source	LaB_6	Field Emission Gun	
Cabling	Multiconductor Cables	Ethernet	
Control	OEM Interface to PDP11/84, VAX	Local Smarts - 3 Internal DEC Alpha CPUs	

Advantages of New System

- 10x Faster Throughput
- One Half Minimum Spot Size
- 2.5 Times Larger Wafers, 1.8 Times Larger Masks
- 3 Times Better Overlay Precision

E-Beam Fabrication of Analog Diffractive Optics

E-Beam Exposure

- For sharp-edged pixels, use multiple E-beam spots for each pixel, low current
  - 2 micron pixels: 10x10 spots/pixel, 9 nA - **7 hrs/cm²**
- For blazed profiles, use few E-beam spots per pixel, high current
  - 1.2 micron pixels: 3x3 spots/pixel, 40 nA - **0.7 hrs/cm²**

Development

- Pure acetone reduces the contrast of the PMMA dose response.
- Acetone is sprayed down onto the spinning sample using a computer-controlled Tridak resist dispense head.
- Additional development patterns (for 633 nm) with dose errors of -5%, 0%, and +5% are added to the chip.
- Development typically starts with 8 seconds and proceeds incrementally in steps as short as 0.5 seconds until the 0%-error development pattern produces a null zeroth order.

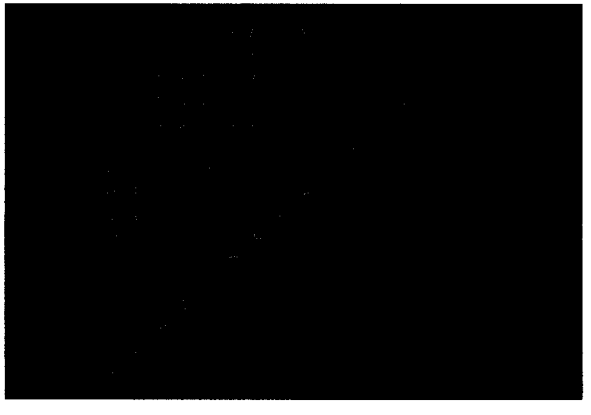

Example Blazed Surface Relief Profiles

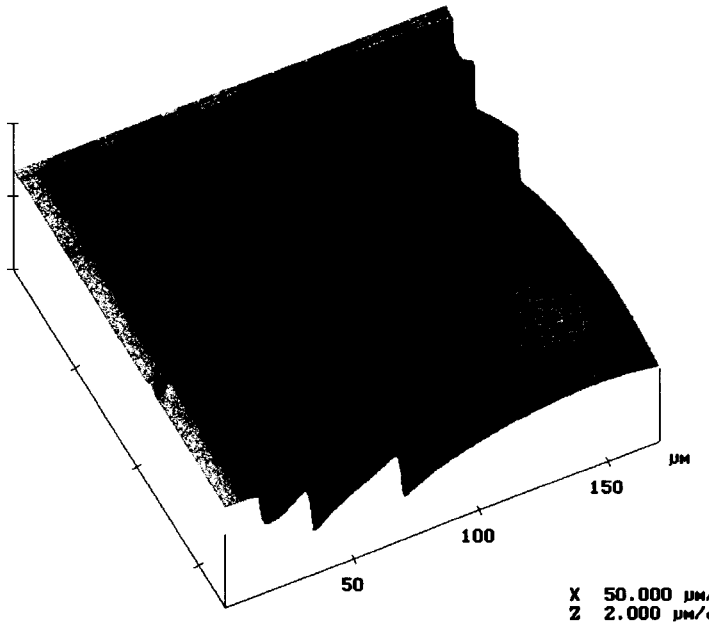

X 50.000 μm/div
Z 2.000 μm/div

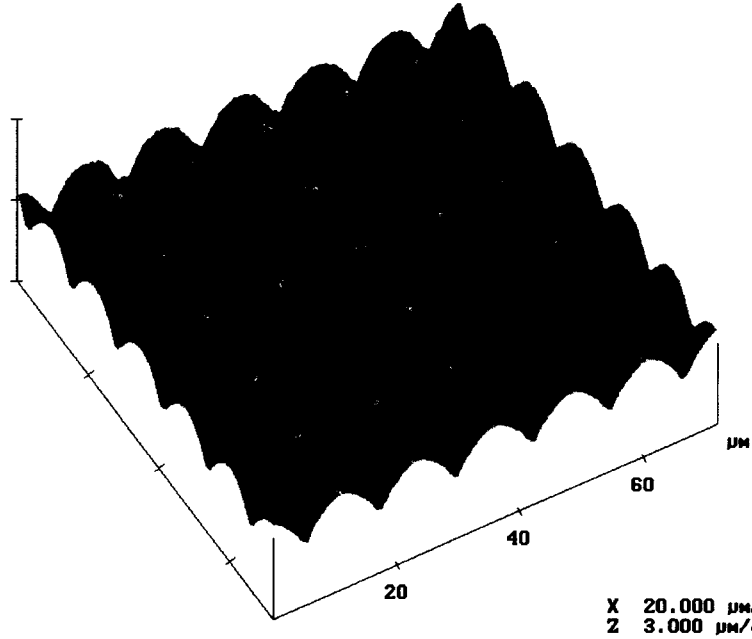

X 20.000 μm/div
Z 3.000 μm/div

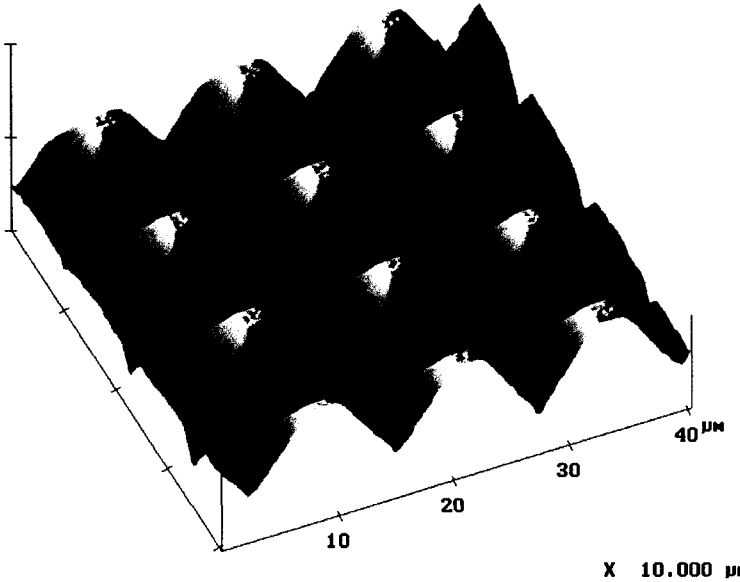

X 10.000 μm/div
Z 1.500 μm/div

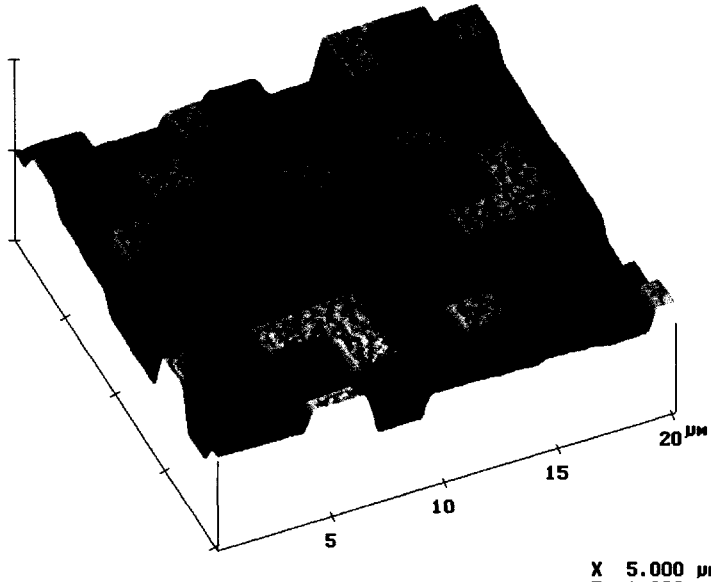

X 5.000 μm/div
Z 1.000 μm/div

Convex Grating Fabrication

- Pattern is broken in to annular sections that cover equal height steps of ~50 microns (E-beam depth of field)
- E-beam *focus, deflector gain, and rotation* are corrected for each annular pattern

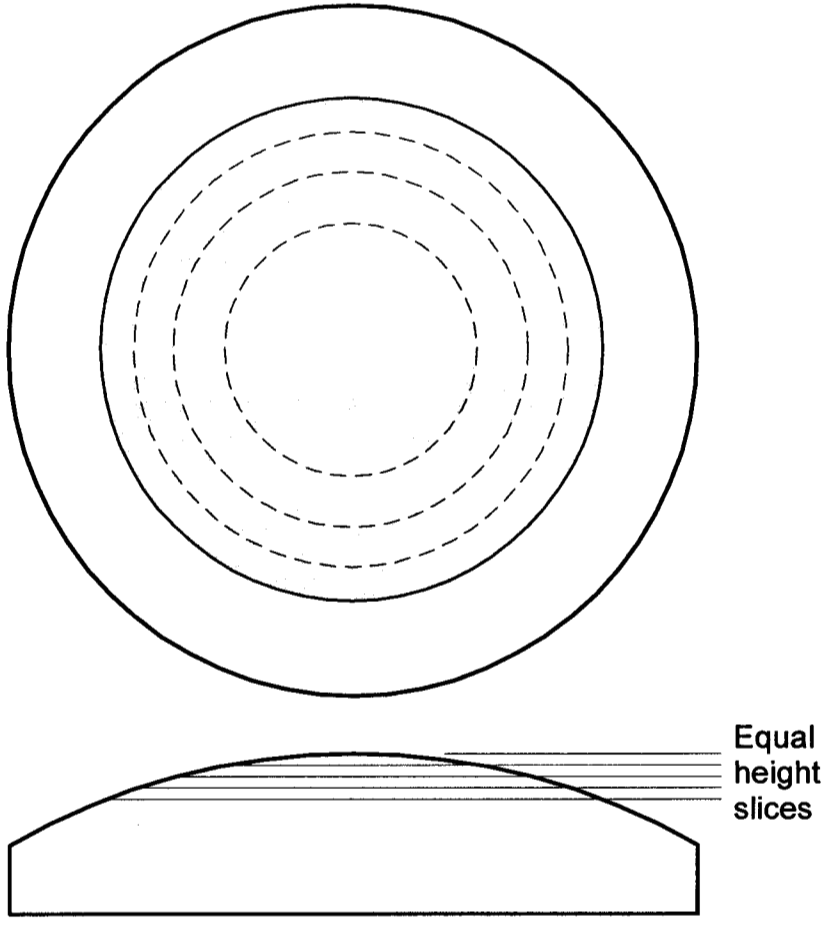

Single-blaze grating on aluminum substrate for *NASA New Millenium EO-1 Mission*

- Selected over diamond-ruled and holographic gratings based on measurements of efficiency, scattering, and wavefront quality

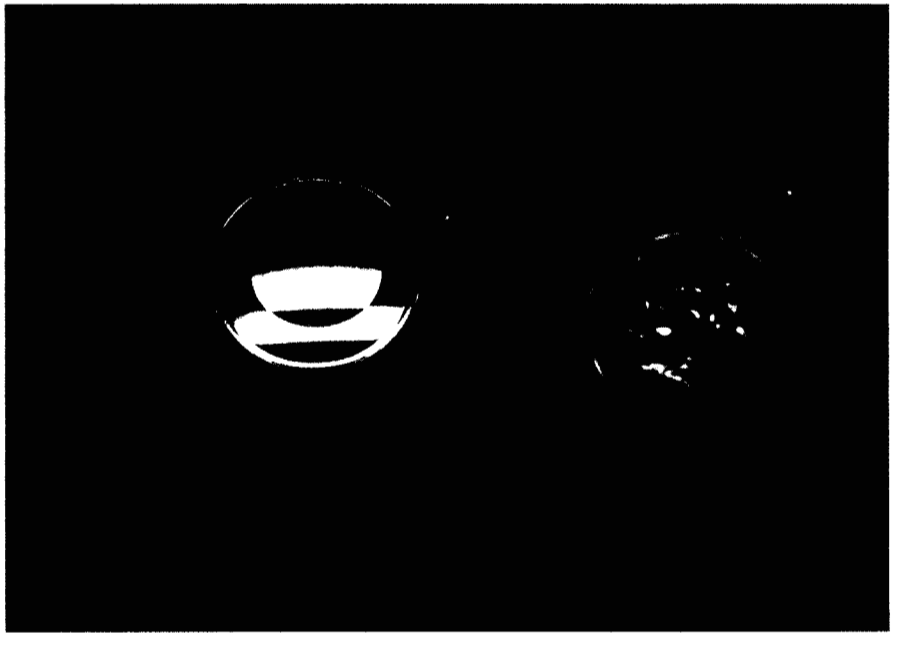

Convex Gratings for Imaging Spectrometers

First-Order Efficiency

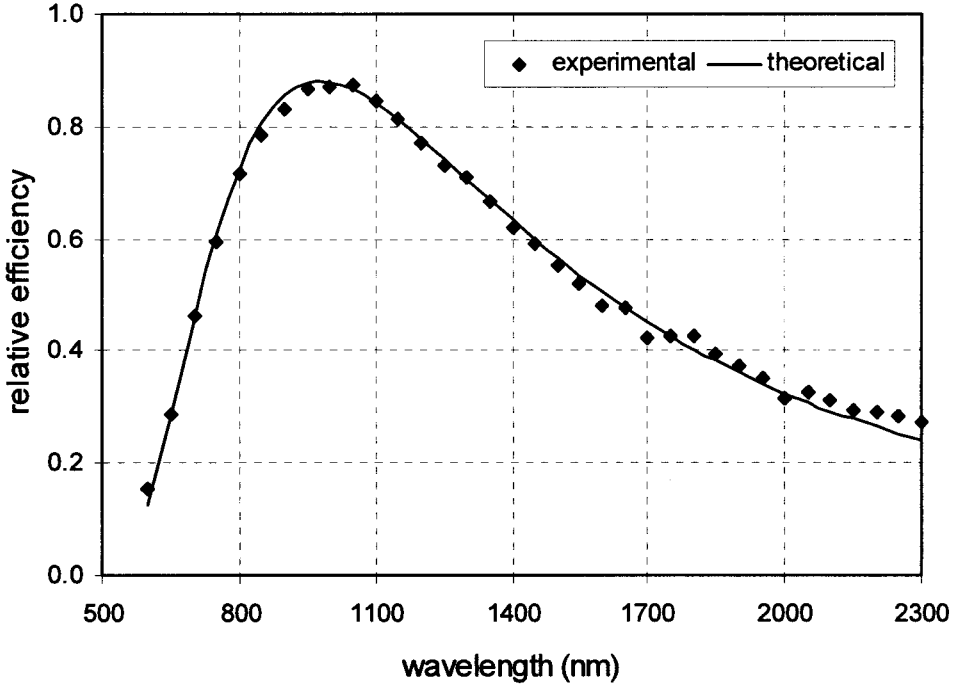

Second-Order Efficiency

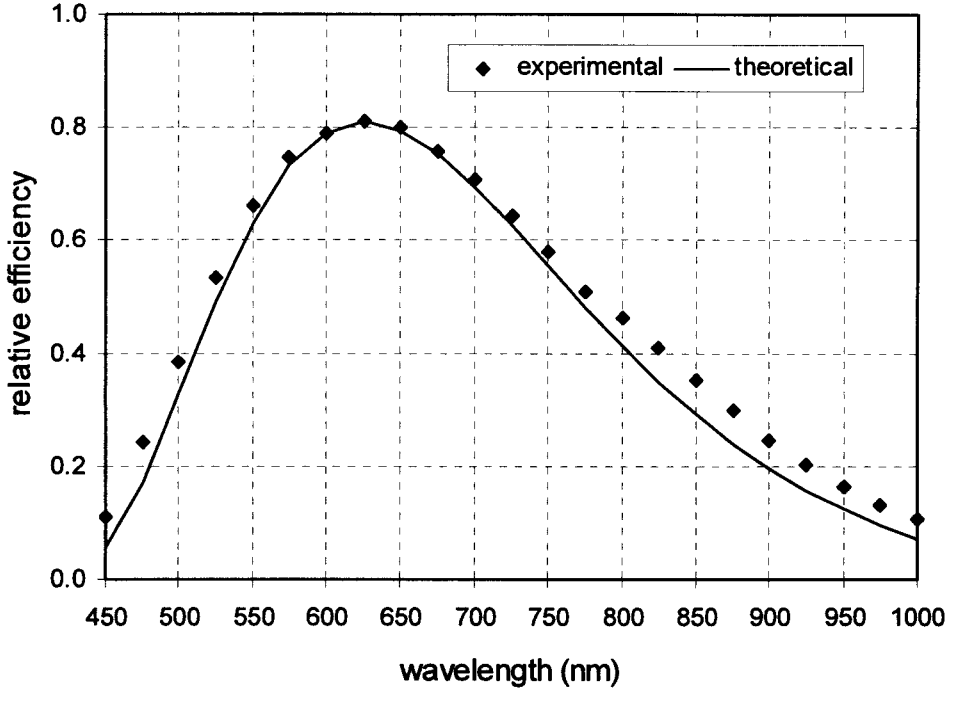

Dual-Blaze Gratings

Dual-Blaze Convex Grating

- Constant period over entire area
- Two blaze angles:
  - center circle blazed for visible
  - outer annulus blazed for infrared
- *High Efficiency for both Visible and Infrared*
- (75% peak, >20% for 0.4 - 2.5 microns)
- Provides flat and high signal to noise ratio.

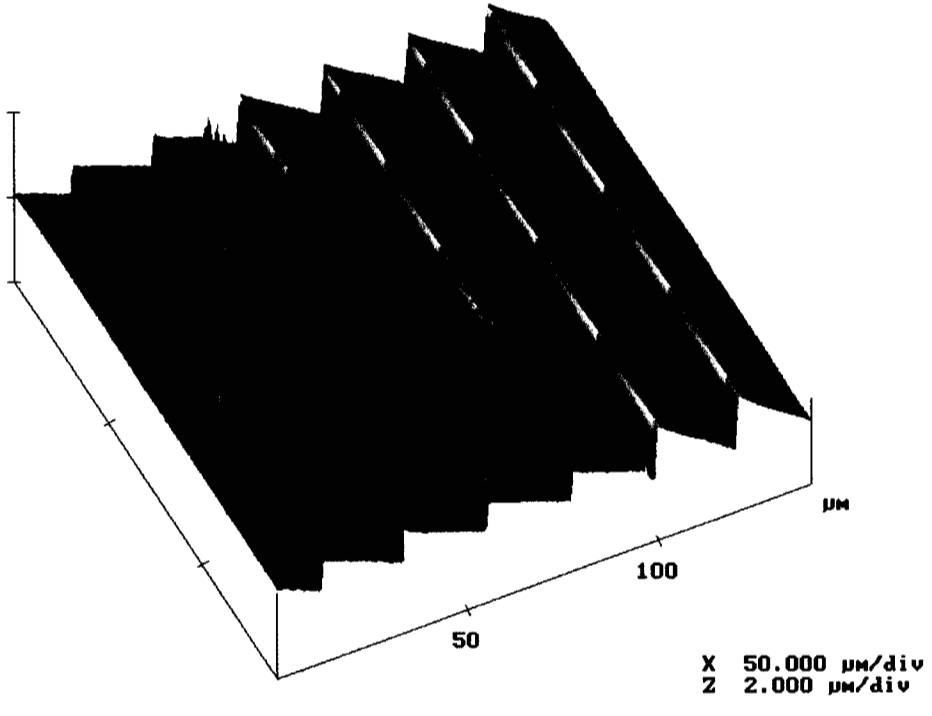

AFM profile of a *dual-blaze* convex grating showing blaze-angle zone boundary

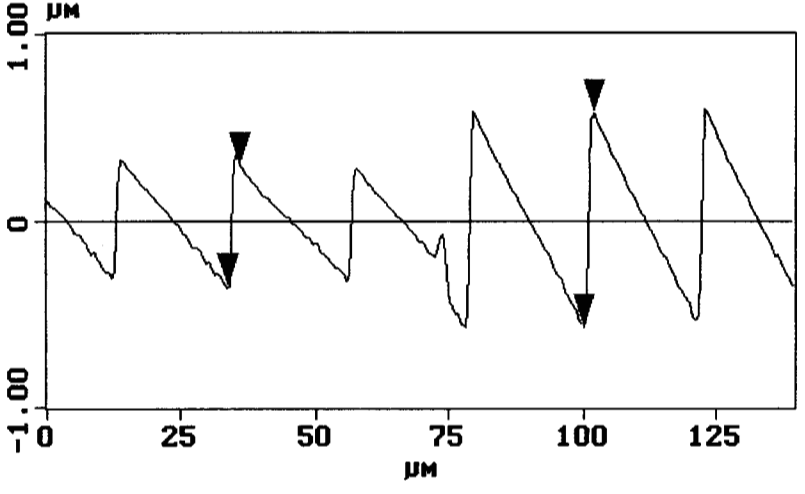

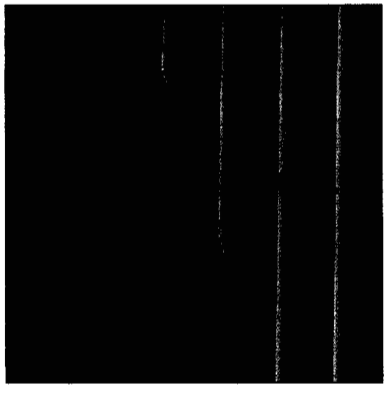

Convex Gratings for Flight-Instruments

Delivered gratings for

- TRW Hyperion (NASA New Millenium EO-1 mission)
- Warfighter (Air Force)

Table 1. Specifications and performance of flight-instrument gratings

Grating	Diameter	Period	Blaze Angle	Substrate Sag	Wavelength range (order)	Peak Efficiency†, Wavelength (order)	Ghosts, Scatter‡
Hyperion VNIR	14 mm	17.4 μm	0.55 deg	0.23 mm	0.4 – 0.85 μm (-1)	92% @ 490 nm	0.025%
Hyperion SWIR	14 mm	17.4 μm	2.27 deg	0.23 mm	1.13 – 2.55 μm (-1)	92% @ 1450 nm	0.16%
Warfighter Dual-band	29 mm	35.7 μm	1.19 deg	1.27 mm	0.5 – 0.85 (-2) 1.0 – 2.45 (-1)	91% @ 0.63 μm (-2) 93% @ 1.26 μm (-1)	0.05%
Warfighter MWIR	36.6 mm	103.6 μm	1.12 deg	0	3 – 5 μm (-1)	Not Meas.	Not Meas.

† - relative to an aluminum mirror

‡ - compared to the brightest order at 633 nm, in all cases ghosts dominated over diffuse scatter

Blazed grating with 0.5 micron period (2000 lines/mm)

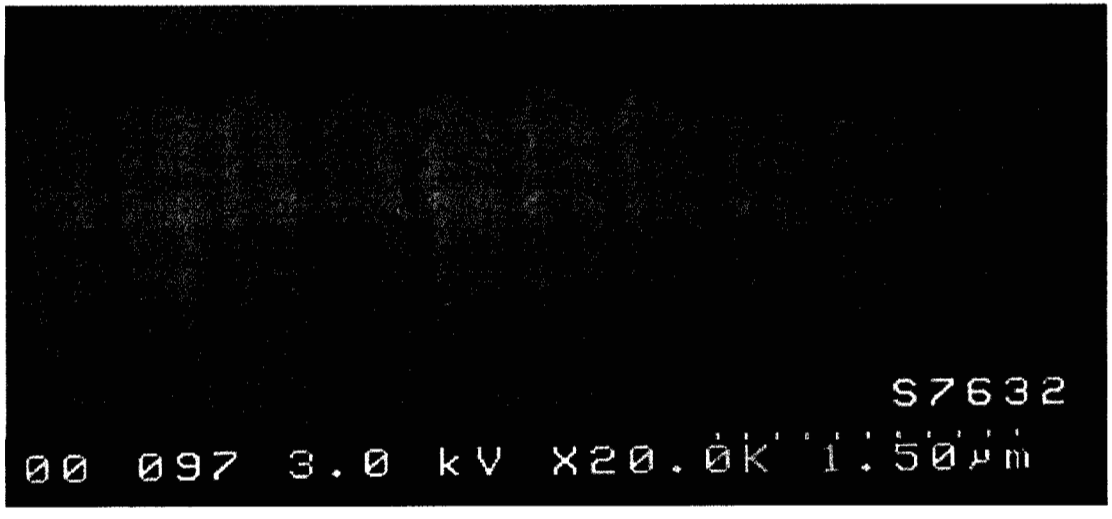

Convex Grating Summary

- Offner imaging spectrometer form is very desirable
- Convex gratings are required
- Direct-write electron-beam fabrication technique works well
- Very high efficiencies
- Need to improve ghosts and scatter (roughness)

Imaging Spectrometry

1. Measure the spectra of all pixels in a scene
2. Analyze the spectra to obtain useful information about the scene

Applications

<u>Remote Sensing</u>

- Mineral exploration
- Hazardous waste monitoring
- Crop/forest health
- Fire/Wetlands monitoring

<u>Defense</u>

- Target identification
- Chemical warfare warning

<u>Biology/Medicine</u>

- Abnormal tissue identification
- Fluorescence studies of cellular processes

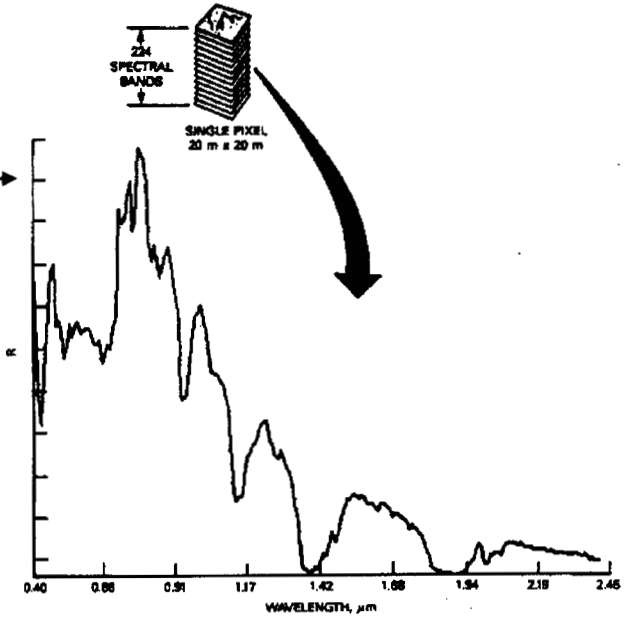

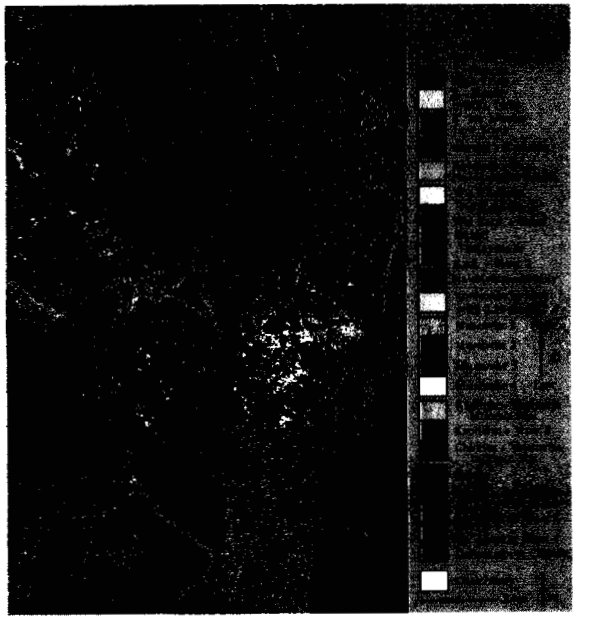

Stationary scene spectral imaging

- Slit imaging spectrometer is used aboard a scanning platform to obtain spectra for a 2D area

Transient scene spectral imaging

- scanning would corrupt data
- computed-tomography imaging spectrometer (CTIS) captures spatial-spectral information for a 2D scene with no scanning

Computed-Tomography Imaging Spectrometer (CTIS)

CTIS enables *transient-event* spectral imaging by capturing spatial and spectral information in a single snapshot

Principle of Operation

- Computer-generated hologram grating splits scene into multiple, spectrally dispersed images
- Tomographic reconstruction yields the spectrum for every pixel in the scene

Advantages

- No moving parts, no scanning of any type
- Simple optical system, can be small and rugged

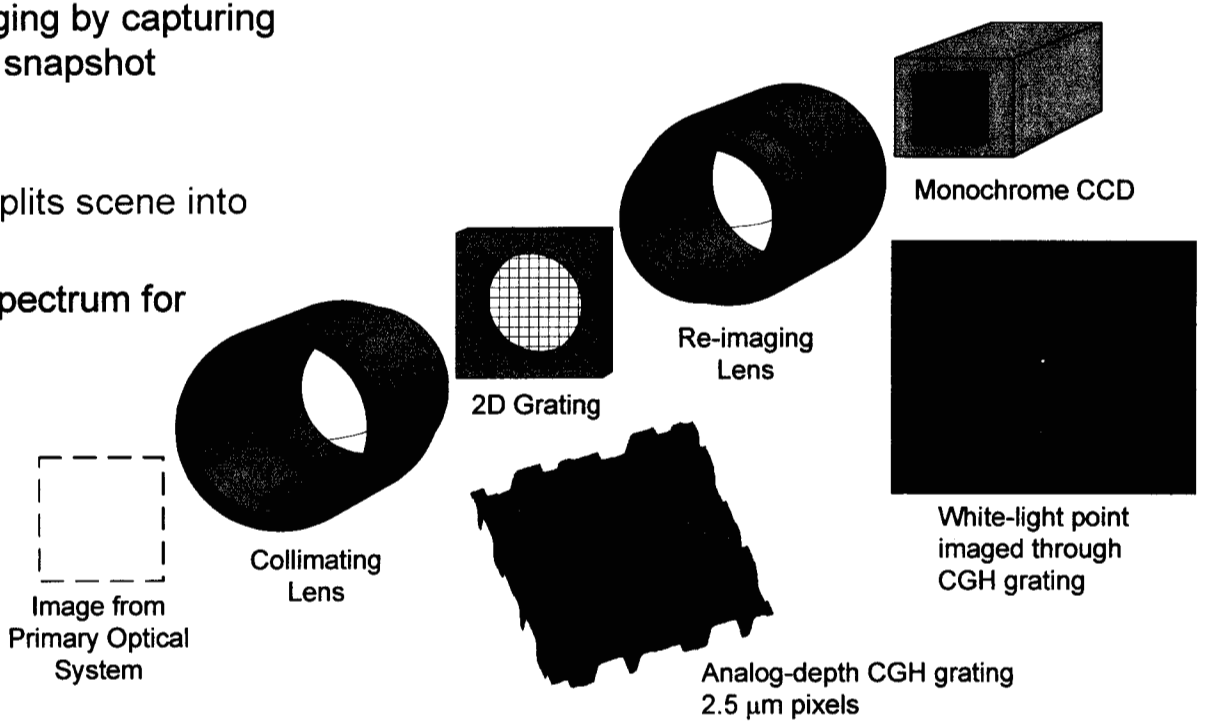

Scene composed of LEDs and laser spots

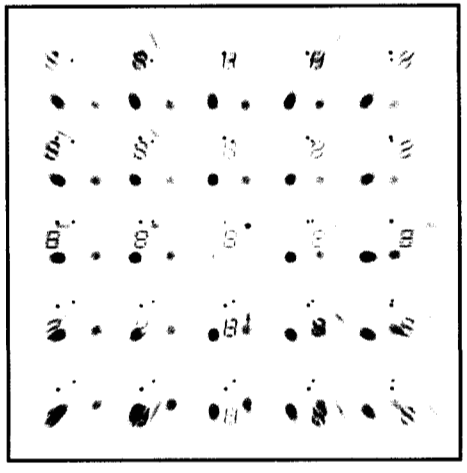

Image captured by CTIS focal plane array (dark ambient)

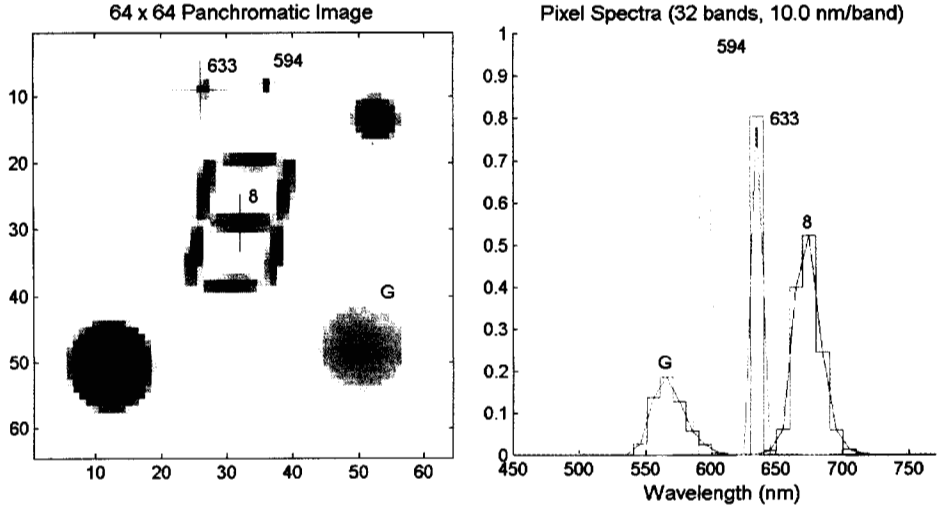

Tomographically reconstructed spatial-spectral information in the scene

Transient-Scene Laboratory Demonstration

- Camera using 1 ms exposure freezes motion of spinning target with colored letters
- CTIS captures spectrally dispersed images and reconstructs spectra of each pixel
- Classification algorithm identifies pixels having common spectra

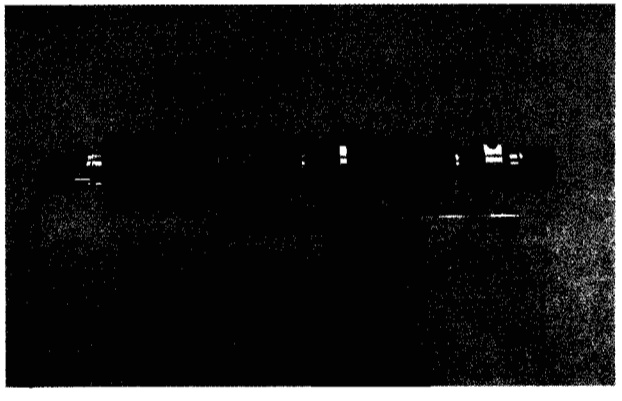

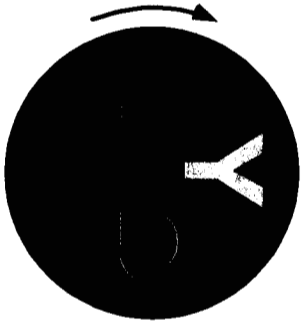

62 x 72 Spectrally Classified Image

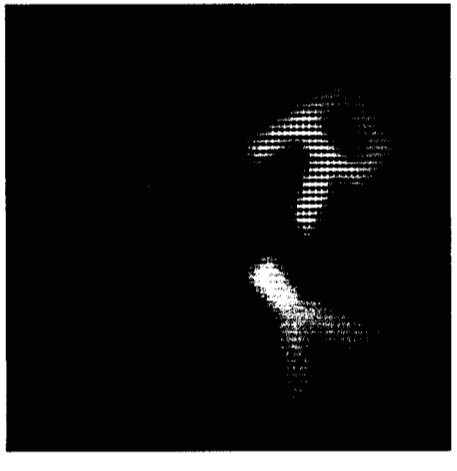

Common Spectra of Bright Pixels

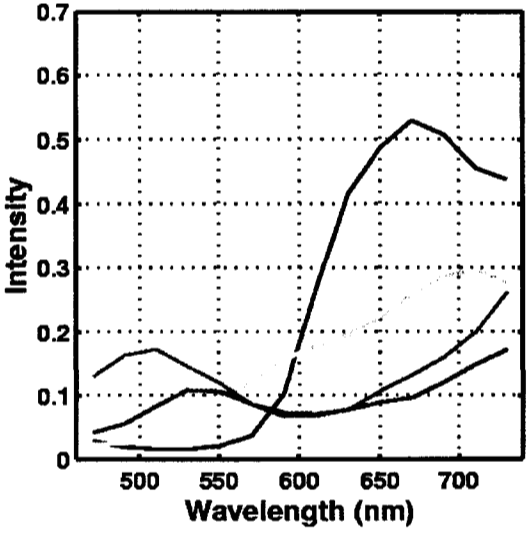

Computer-Generated Holograms

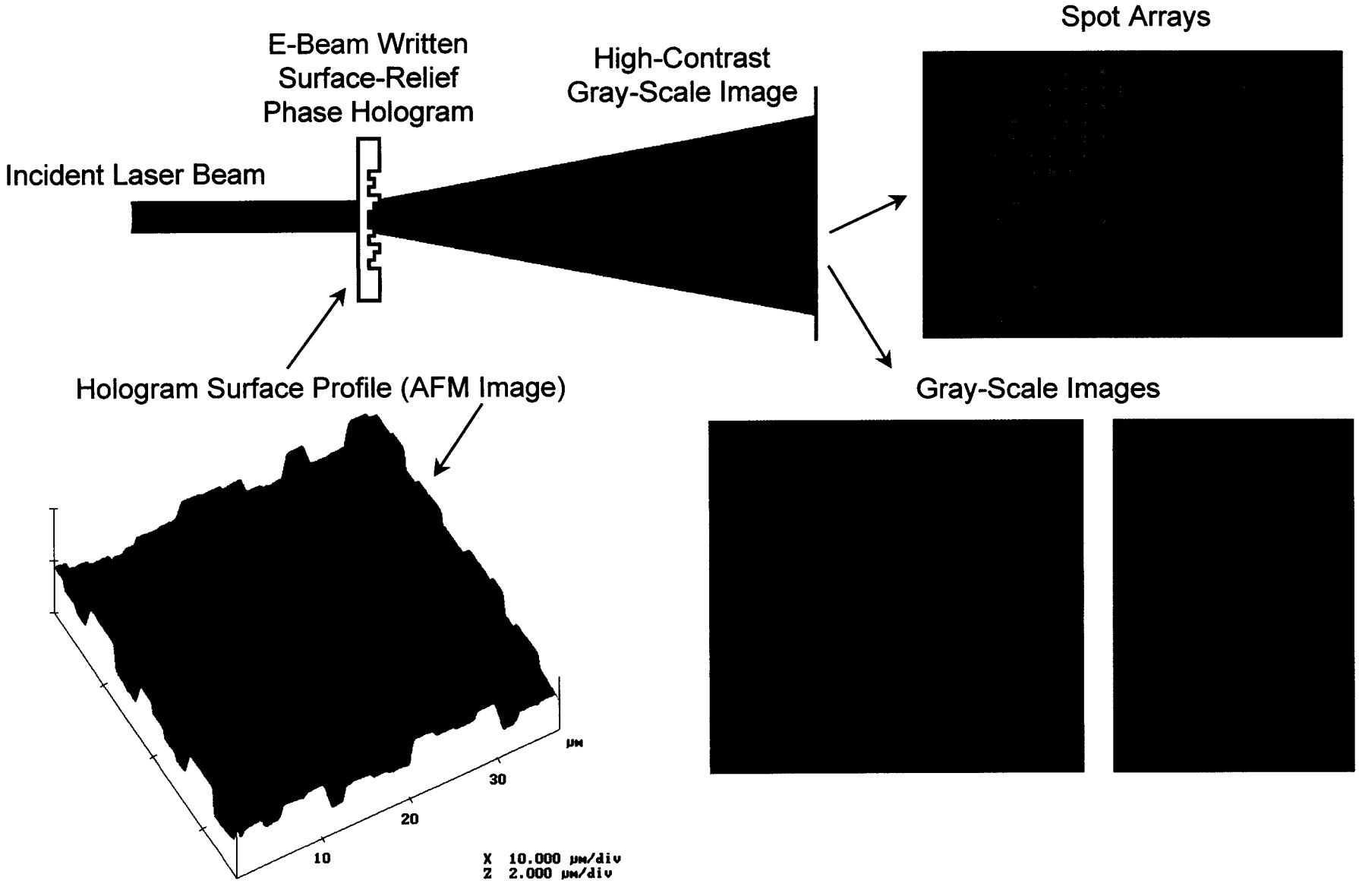

Computer Generated Hologram 2-D Grating Design for CTIS

Goals

- Avoid saturation of the detector by the zeroth (undiffracted) order
- Fill focal plane array with diffracted orders
- Weight diffraction efficiencies to compensate for dispersion
- Produce balanced diffraction efficiency thoughout the wavelength band

Approach

- CGH 2D disperser
- Infinite design space for analog depth profiles
- Perform many Gerchberg-Saxton iterative designs for a single wavelength
  - Simulate performance at many wavelengths
  - Choose best design according to a merit function
- Use singular value decomposition algorithm to design constrained CGH

CGH grating designed by Gerchberg-Saxton algorithm

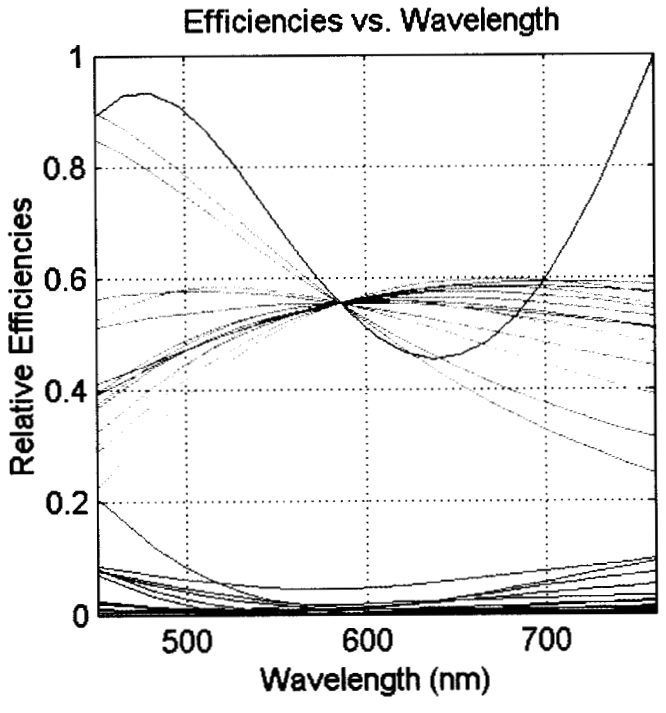

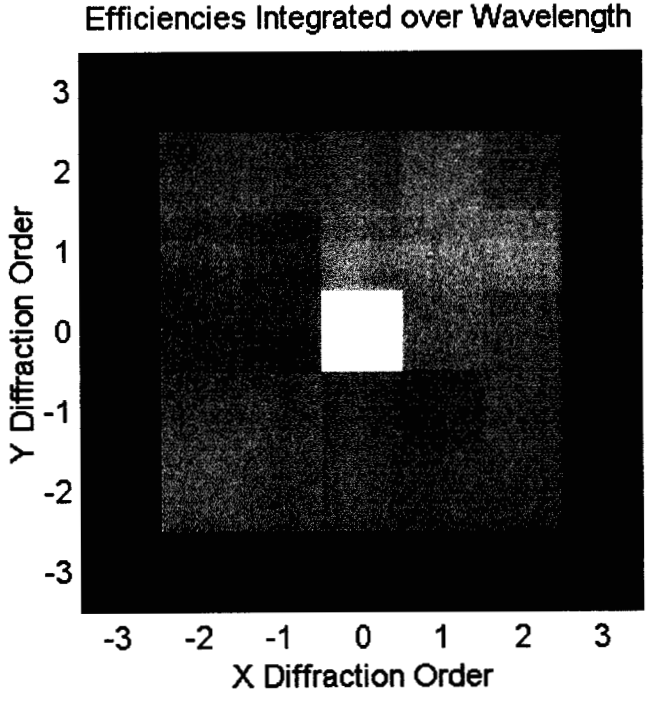

CGH grating designed by Singular Value Decomposition

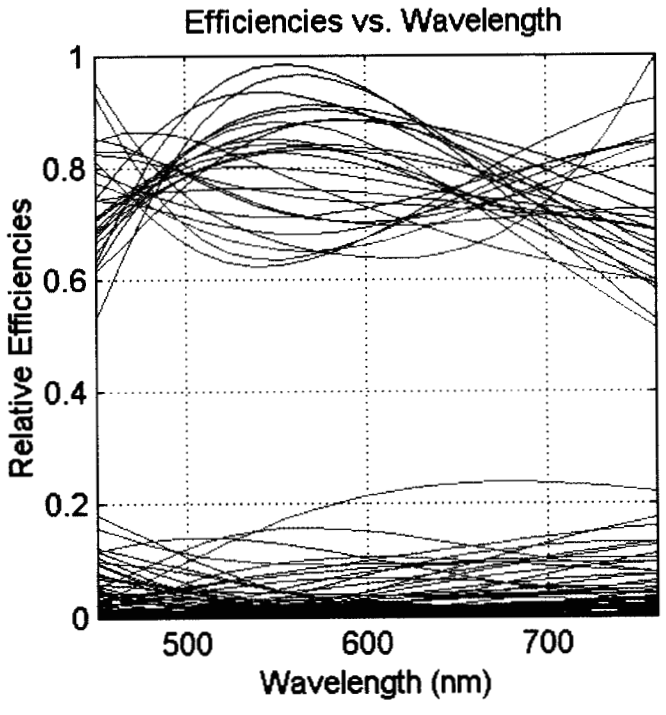

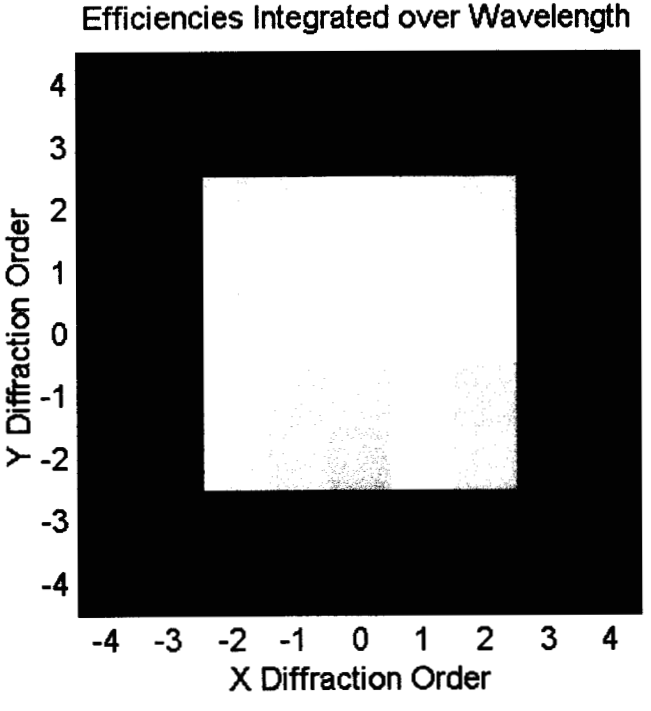

CTIS Grating Summary

- CGH gratings for CTIS must perform well over a wide wavelength range
- E-beam fabricated CGH gratings have demonstrated good broadband performance
- Ultimate CTIS grating design is still unknown

Conclusion

- Novel imaging spectrometers require state of the art diffractive optical elements
  - Convex blazed gratings
  - Broadband CGH 2D gratings
- Electron-beam lithography is a flexible tool for fabricating such gratings
  - Non-flat substrates (convex or concave, aspheric)
  - Very efficient blazing
  - Non-straight grooves
  - Roughness can be improved
- CTIS grating design problem has not been fully explored